A R T I C L E S

Functional and Cellular Responses in a Novel Rodent Model of Anterior Ischemic Optic Neuropathy

Steven L. Bernstein,[1,2,3] Yan Guo,[1] Shalom E. Kelman,[1] Robert W. Flower,[1] and Mary A. Johnson[1]

PURPOSE. Anterior ischemic optic neuropathy (AION) is caused by sudden loss of vascular supply to retinal ganglion cell (RGC) axons in the anterior portion of the optic nerve and is a major cause of optic nerve dysfunction. There has been no easily obtainable animal model of this disorder. The current study was conducted to design a novel model of rodent AION (rAION), to enable more detailed study of this disease.

METHODS. A novel rodent photoembolic stroke model was developed that is directly analogous to human AION. Using histologic, electrophysiological, molecular- and cell biological methods, the early changes associated with isolated RGC axonal ischemia were characterized.

RESULTS. Functional (electrophysiological) changes occurred in RGCs within 1 day after rAION, with a loss of visual evoked potential (VEP) amplitude that persisted in the long term. The retinal gene expression pattern rapidly changed after rAION induction, with an early ($<$1 day) initial induction of c-Fos mRNA, and loss of RGC-specific gene expression. RGC-specific protein expression declined 2 days after detectable mRNA level changes, and immunostaining suggested that multiple retinal layers react to isolated RGC axonal ischemia.

CONCLUSIONS. rAION rapidly results in electrophysiological and histologic changes similar to clinical AION, with reactive responses in primary and supporting neuronal cell layers. The rAION model can enable a detailed analysis of the individual retinal and optic nerve changes that occur after optic nerve stroke, which may be useful in determining possible therapeutic interventions for this disorder. (*Invest Ophthalmol Vis Sci.* 2003;44:4153–4162) DOI:10.1167/iovs.03-0274

In vertebrates, processed retinal signals are sent through the optic nerve (ON) to higher regions in the central nervous system (CNS). Retinal ganglion cell (RGC) axons comprise the ON, with a cell soma in the retina.[1] RGCs are typical CNS myelinated long-axon neurons. Unlike other CNS neurons, however, the blood supply of the RGC axon in the ON is distinct from that supplying the RGC cell body. Anterior ischemic optic neuropathy (AION), the most common type of acute ION, results from microvascular thrombosis at the junction of the ON and retina.[2] AION clinically presents with painless loss of vision in the affected eye, ON swelling (disc edema), and disruption of the normal nerve architecture,[2] resulting in RGC death through apoptosis and permanent vision loss.[3] Because RGCs are CNS neurons, AION resembles other white-matter CNS stroke events. Thus, cellular responses in AION are directly relatable to the general problem of CNS axonal ischemia.

Numerous models have been created to identify the RGC response to ON damage, including ON crush,[4] transection,[5] increased ocular pressure,[6] and infusion of vascular constricting agents.[7] However, none of these models resembles the natural course of AION, or CNS ischemic axonopathy in general. We therefore developed an easily utilizable, photothrombosis-induced rat model of AION (rodent AION, or rAION), which resembles the functional, histologic, and physiologic defects seen in the human disease.

We selectively thrombosed the microvessels supplying the ON, by directly illuminating the intraretinal portion of the ON with a laser, after intravenous infusion with the photosensitizing agent rose bengal (RB), a derivative of fluorescein dye. RB is activated by visible light to generate superoxide radicals.[8] Photoactivation of intravascular RB selectively damages the vascular endothelium, producing thrombosis while sparing nonvascular tissues.[9–12] The RB-photoactivation technique has been demonstrated to cause retinal vascular thrombosis only in areas of direct light exposure.[12] A study has also demonstrated that it is superoxide radicals, rather than direct thermal damage, that are the primary cause of light-induced, RB cellular toxicity.[13] Although superoxide radicals are toxic to all vascular membranes, appropriate RB exposure times can thrombose capillaries supplying just the ON, while sparing the larger caliber central retinal vessels that pass through the ON and supply the inner retinal circulation. The rAION model is thus directly analogous to human AION. We used this method to determine the in vivo RGC and ON response to rAION, without significant intraretinal damage or disturbance of underlying retinal structures.

METHODS

rAION Induction

All animal protocols were approved by the University of Maryland at Baltimore (UMAB) institutional animal care university committee (IACUC), and adhered to guidelines recommended by the ARVO Statement for the Use of Animals in Ophthalmic and Vision Research. Male Sprague-Dawley rats (130–150 g; Charles River, Wilmington, MA) were anesthetized with ketamine/xylazine (80 mg/kg and 4 mg/kg, respectively). Sham surgery consisted of ON/retinal region illuminated with

TABLE 1. Oligonucleotide Primer Sequence and Conditions Used in Semiquantitative rt-PCR Analysis of mRNA Levels

Gene	Accession No.	Primer Sequence (5′–3′)	T_{ann} (°C)	Fragment Size (bp)	Cycles (With Control Primer)	Control/ Competimer Ratio
C-Fos	S06769	For: ACG CGG ACT ACG AGG CGT CAT Rev: CTT CGG ATT CTC CGT TTC TC	58	411	29	1:7
Brn 3.2	S68377	For: AAG CGC AAG CGC ACG TCC ATC Rev: AAA AGA GGC AGA AGA GAC AAG A	55	272	27	1:9
HSP84	S45392	For: TGA TGC CCT GGA CAA GAT TCG Rev: ATA CTG CTC ATC ATC GTT GTG	62	321	21	1:4
HSP86	AA944397	For: CTC ATT CCC AAC AAG CAA GAC CG Rev: TGG TTC ACC TGT GTC TGT CCT	60	300	23	1:4
Opsin	U22180	For: TGG TGC GCA GCC CCT TTG AGC Rev: GCG GAA GTT GCT CAT GGG CTT	63	385	16	3:2
HSP70-1/2	X77207	For: TCC AGC ACG GCA AGG TGG AGA Rev: CGT TGA TGA TCC GCA GCA CGT	65	453	21	1:5

Gene and accession numbers are indicated. Oligonucleotide primer sequences are shown in the 5′ direction. Primer annealing temperatures (T_{ann}) and predicted fragment sizes are shown. The ratio of 18s rRNA internal standard primer and competimer used for each reaction type are indicated, as are the number of PCR cycles following initial (94°C; 2 minutes) denaturation, to generate a nonsaturating product comparison. For, forward; Rev, reverse.

argon laser light (514 nm) or frequency-doubled yttrium-aluminum garnet laser (YAG, light 535 nm; Iridex, Mountain View, CA) without RB. To induce rAION, RB (90% purity; Sigma-Aldrich, St. Louis, MO) was administered intravenously through the tail vein using a 28-gauge needle (2.5 mM RB in phosphate-buffered saline [PBS]/1 mL/kg animal weight). After administration of RB, the rat ON was directly treated with an argon green 514-nm/500-μm spot laser (Coherent, Palo Alto, CA) for 20 seconds. After treatment, retinas were examined and photographed (T320; Eastman Kodak, Rochester, NY; or D1X digital camera at 2.3 megapixels, ASA 800, incandescent; Nikon, Tokyo, Japan).

Histologic Preparation

Retinal tissue for histologic analysis was fixed in either 4% paraformaldehyde-phosphate-buffered saline (PF-PBS) or methacarn and paraffin embedded. Six-micrometer sections were step-cut through rAION-treated and control eyes, and cells in the RGC layer, as well as the number of cell layers in the inner (INL) and outer (ONL) nuclear retinal layers, were counted (12 high-power fields per retina). Statistical analysis was performed ($n = 5$ animals/group) comparing total number of RGCs per section and the relative thickness in cell layers of the INL and ONL, in each test group for both treated and contralateral eyes, using Student's two-tailed t-test.

Visualization of Optic Nerve Circulation

To confirm the ischemic nature of the RB laser-induced ON lesion, control animals, and animals 30 minutes after rAION induction were terminally anesthetized with 50 mg/kg pentobarbital (Nembutal; Abbott Laboratories, Abbott Park, IL). The inferior vena cava was incised, and the left ventricle was rapidly perfused with 5 mL India ink through a 19-gauge intracardiac needle. The mouse was decapitated 10 seconds after beginning perfusion. This technique results in filling of all capillary beds (retinal, choroidal, and iris) with India ink before decapitation, allowing tracing of patent vessels. After death, eyes were dissected, and postfixed in 4% PF-PBS for 24 hours. Retinas were dissected, along with the choroidal vasculature immediately adjacent to the ON, flatmounted with aqueous mounting medium (Crystal/Mount; Biomeda Corp., Foster City, CA) and photographed.

Immunohistology and Optic Nerve Analysis

Optic nerve tissue was fixed in glutaraldehyde-paraformaldehyde fixative and embedded in Epon. Sections (0.5-μm-thick) of control and rAION-treated nerves were stained with toluidine blue. Immunohistology was performed with rabbit polyclonal antibodies specific for HSP84 and -86 proteins (ABR, Golden, CO) at a 1:100 dilution. Brn 3.2 antibody (Santa Cruz Biotechnology, Santa Cruz, CA) was used at 1:25

dilution. Sections were developed with a kit (Vectastain elite; Vector Laboratories, Burlingame, CA) and 3-amino-9-ethylcarbazole (AEC) reagent.

Physiological Testing

Optic nerve function was evaluated on ketamine and /xylazine (80 mg and 4 mg/kg, respectively) anesthetized animals, through visual evoked potential (VEP). The fellow eye was covered with an opaque contact lens during testing. The stimulus was a 2 Hz, 1.95-cd s/m^2 Ganzfeld strobe flash; 80 responses per eye were averaged. Band-pass cutoff frequencies were 0.3 and 100 Hz. The occipital (visual) cortical response was measured using electrodes placed on the shaved skull. The untreated (control) eye of each animal was used for internal comparison.

RNA Isolation and Gene Expression Analysis

Animals for RNA analysis were killed with CO_2 inhalation. Retinal tissue was immediately dissected and stored at -70°C until use. RNA was extracted (RNAzol B; Tel-Test, Friendswood, TX). First-strand cDNA was generated from total RNA using a kit (Retroscript; catalog no. 1710; Ambion, Austin, TX). We characterized changes in mRNA levels of six genes, using a two-step, multiplex, semiquantitative reverse-transcriptase–based polymerase chain reaction (rt-PCR). Quantification of selected genes was compared using simultaneous amplification of the test gene, and an 18s ribosomal RNA loading standard (18s rRNA) cDNA product to compensate for tube-to-tube variations in RNA loading and PCR reactions. Because cellular 18s rRNA concentration is at least two orders of magnitude greater than individual messengers, 18s rRNA-cDNA product for each reaction was quantitatively inhibited by a selective competitive inhibitor of the 18s rRNA product (Competimer Technology; Ambion). The ratios of 18s rRNA primer and competimer were optimized for each test gene primer pair (Table 1), to ensure that both the gene of interest and 18s rRNA product are measurable within the linear quantitation range. Gene expression profiles were compared between individual control (RB/no rAION induction) and rAION-induced retinal pairs. Gene-specific oligonucleotide primers were generated for individual rat sequences. These are seen in Table 1. The studied genes c-fos, brn3.2, HSP70-1/2, opsin, HSP86, and HSP84 were chosen because: (1) c-fos is an indicator of immediate early tissue stress[14,15]; (2) brn3.2 is expressed specifically in the retina by RGCs[16]; (3) HSP70-1/2 is a tissue stress-induction marker used in many systems[17]; (4) HSP86 and -84 play major roles in RGC axonal function[18]; and (5) rod opsin is an indicator of outer retinal cell layer function and photoreceptor damage.[19]
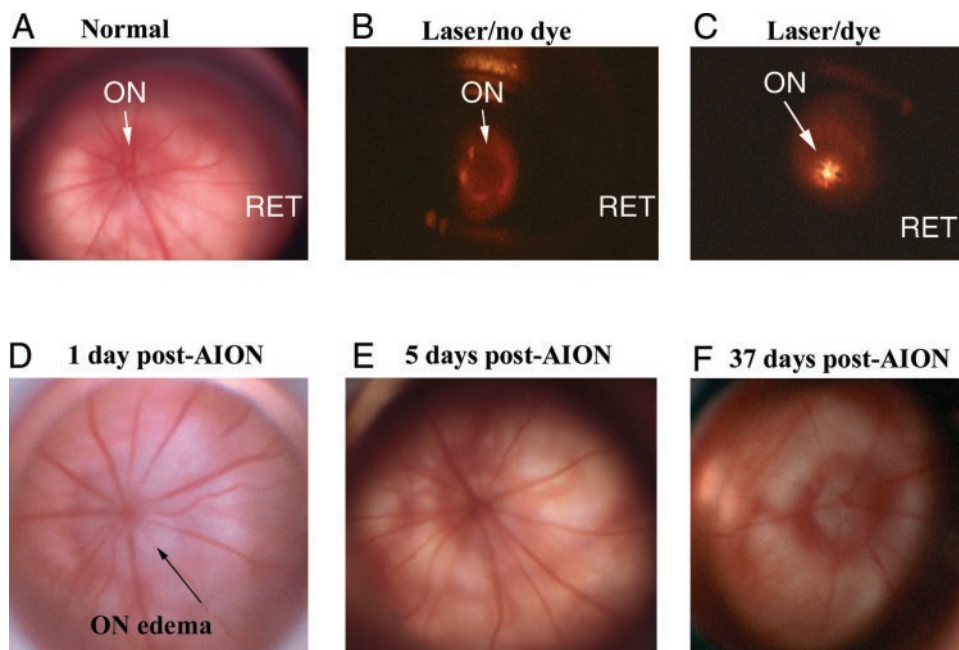
FIGURE 1. (**A**) Normal (control) ON photographed by slit lamp. The ON contains the central retinal vessels (*arrow*) that emerge to supply the inner layers of the retina (RET). (**B**) Sham operation (laser illumination/no RB). (**C**) ON and retina illuminated with laser light (514 nm) after pretreatment with RB. Fluorescence was limited to vessels in the region of laser exposure (the ON). Appearance of the ON (**D**) 1 day after rAION induction. *Arrow*: NFL. (**E**) Five days after rAION induction; ON edema had resolved. (**F**) Thirty-seven days after rAION induction, the ON was pale and reduced in size. Magnification, ×17.

PCR-amplified fragments were sequenced to ensure identity. The brn 3.2 rat homologue was not available; nucleotide and peptide sequence data were compared from both mouse (brn 3.2; accession number S68377) and human brn 3b (U06233) homologues. Brn 3.2 oligonucleotide primers were prepared from conserved (human+mouse) nucleotide regions, and used to amplify a product from rat retina mRNA. The amplified fragment was sequenced and found to be 98.4% identical with mouse brn 3.2 mRNA sequence. Five-pairs per time point were used and a statistical test for significance was performed with Student's two tailed *t*-test.

RESULTS

Effect of rAION on the Appearance of ON and Retina

In rats, radial central vessels emerged from the ON (Fig. 1A, arrow) to supply the inner retina (Fig. 1A; RET). The normal ON–retina border was demarcated with a surrounding reddish hue (Fig. 1A). The ONs of the sham-operation animals under laser illumination without RB pretreatment were dark (Fig. 1B). In contrast, exposure of the ON to laser light after RB administration produced vascular fluorescence only within the diameter of the light exposure (Fig. 1C). No fluorescence was seen when the ON was re-exposed to laser light 15 minutes after treatment (data not shown), suggesting that RB remains within the retinal and ON vasculature and does not leak into the surrounding tissues.

One day after rAION induction, the ON was pale and swollen (Fig. 1D). The ON–retina border was blurred by nerve fiber layer (NFL) edema (Fig. 1D; arrow). No change was seen in the ONs of animals exposed to laser illumination without RB (data not shown). ON edema decreased 3 days after induction (data not shown) and resolved by 5 days after induction (Fig. 1E; compare with Figs. 1A and 1D). The 5-day nerve appeared grossly normal. However, the ON at 37 days after induction was pale and shrunken (Fig. 1F). In contrast, there was no change in the appearance of the ON of dye alone, the laser-treated control, or naïve animals after the same time intervals (data not shown). The ON changes in rAION changes mirrored the clinical course of AION, which typically produces long-term ON pallor and shrinkage of the ON.[20]

Effect of RB-Laser Induction Technique on Capillaries Supplying the ON

The rat ON is perfused by capillaries derived from the central retinal vessels, as well as recurrent choroidal vessels surrounding the nerve.[21] Optic nerve capillary filling by India ink is seen in Figure 2. In the sham-treated (laser/no dye) eye, many intraretinal capillaries supplied by the central retinal vessels were visible (Fig. 2A, small arrow). Within the ON (Fig. 2B), there were many small capillaries. These are visible within the circle of the choroidal vessels that define the ON borders (Fig. 2B, large arrow). No difference was seen in filling characteristics of naïve control or RB-treated/no laser animals compared with sham-treated animals (data not shown). The intraretinal capillaries of rAION-induced animals (30 minutes after induction) away from the ON also fill with India ink (Fig. 2C, arrow), although there was incomplete filling of vessels close to the central vessels of the ON (Fig. 2C). Examination of circulation within the ON of rAION animals showed a severe reduction in the filling of many of the ON capillaries (Fig. 2D). Choriocapillary filling was clearly demarcated (Fig. 2D, double arrows), with few recurrent vessels visible between the central retinal vessels and choriocapillaris (Fig. 2D). Thus, the ON defect induced by the RB-laser technique is a true ischemic lesion.

rAION-Induced Changes in ON Function

After AION, the human ON's ability to conduct electrical signals decreases, as measured by a loss of amplitude in the VEP.[22,23] VEPs generated from treated eyes (Figs. 3A–D, dotted traces) were compared with responses from the control eyes (Figs. 3A–D, solid traces). VEP results vary widely between individuals,[23] but are internally consistent between eyes of the same individual at the same testing session. Thus, amplitude differences between individuals are not comparable, and only differences between control and experimental eyes in a given individual can be measured.

Although treatment exposure was not standardized in this study, the median amplitude reduction in the treated eye was 20%. No change was seen in non-RB, laser-treated eyes when compared with the control (Fig. 3A, rat A). VEP responses from individual rAION-affected animals always were reduced, com-
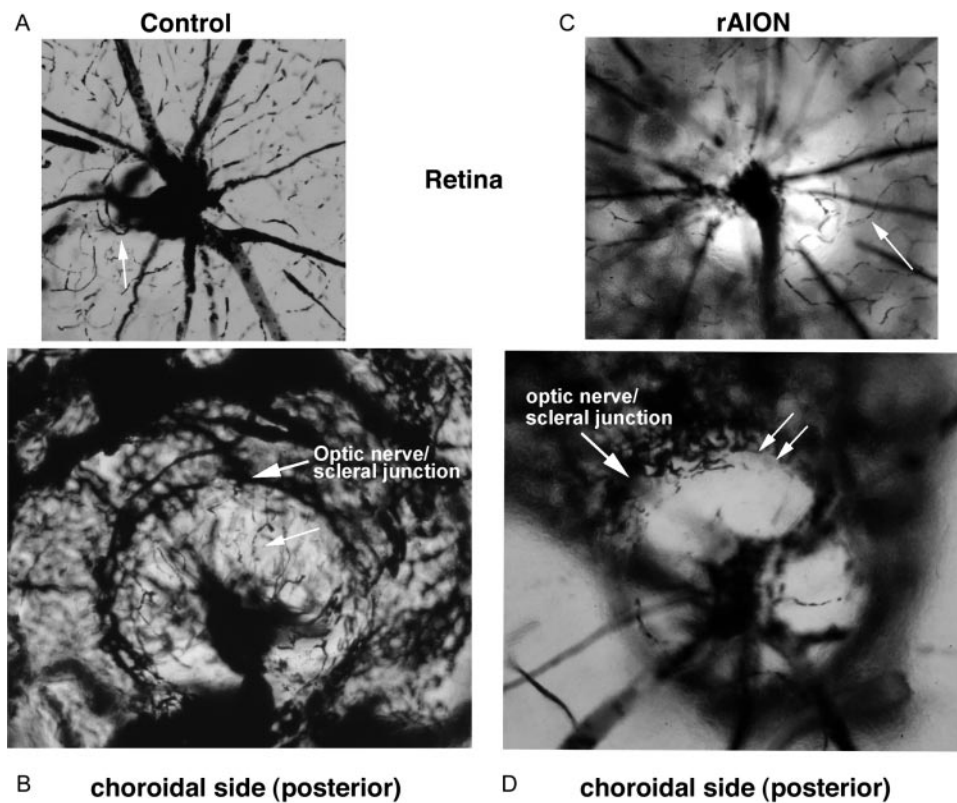
FIGURE 2. Retina, ON, and choriocapillaris patency evaluated by India ink perfusion in vivo. Living animals were perfused with India ink, and immediately after perfusion, animals were decapitated, the sclera and choroid were dissected farthest from the ON, and the retina and retina–ON junction were flat-mounted and photographed. (**A**) The intraretinal vasculature of sham-treated eye (dye/no laser). Intraretinal capillaries were clearly visible as a net around the ON and between the major intraretinal vessels. Capillaries supplying the ON region were also seen (*arrow*). (**B**) Close-up view of the capillaries supplying the ON from the posterior side of the retina (choroidal side). The ON junction appeared as a dark circle around the central retinal vessels. Many capillaries were present within the ON area (*arrow*) and also emanated from the ring of the choriocapillaris surrounding the ON. (**C**) Intraretinal circulation 30 minutes after rAION induction. There was a reduction in the apparent number of intraretinal capillaries close to the ON (★★), with sparing of capillaries farther from the disc (*arrow*). (**D**) Anterior ON circulation 30 minutes after rAION induction. There was nonperfusion of many capillaries supplying the ON (*pale circle*). A single capillary was visible within the lower right quadrant of the ON. The choriocapillaris circulation (outside the circle of the ON) was patent, but with loss of recurrent capillaries to the nerve (*double arrow*). Magnification, ×250.

pared with control eyes, but the level of reduction varied between animals. VEP differences between rAION-affected and control eyes in individual animals ranged from 17% (Fig. 3C, rat C) to 70% (Fig. 3B, rat B). These VEP amplitude differences between treated and untreated eyes are statistically significant (two tailed paired t-test; $P = 0.015$; $n = 16$; $t = -2.77$).

The VEP amplitude depression at early times after rAION induction (e.g., Fig. 3C, rat C; 3 days) continued even 45 days after induction (e.g., Fig. 3D, rat C; 45 days; dotted trace). No statistical analysis was performed at the latter time point, due to the low number of subjects. Thus, rAION produces a loss of ON electrical function, with permanent degradation of normal ON electrical activity.

rAION-Induced Histologic Changes in the Retina and ON

RGCs are present as a single cell layer in the rodent retinal (Fig. 4D; RGC), and their axons compose the NFL (Fig. 4D). NFL axons form the ON (Fig. 4A; ON). The intraretinal portion of the ON was triangular in appearance and flat against the retinal surface (Fig. 4A, arrow), with little extrusion into the intraretinal compartment. One day after treatment, no changes in ON–retinal junction histology were seen in animals exposed to either laser illumination alone (Fig. 4A) or RB dye alone (data not shown). The NFL was triangular in appearance, with no displacement of the peripapillary retina (Fig. 4A, arrow). In contrast, NFL swelling anterior to the site of ON ischemia resulted in ON edema, 1 day after rAION induction, (Fig. 4B, double asterisks). Optic nerve edema was also apparent from the displacement of the peripapillary retina (Fig. 4B, double arrows). Thirty-seven days after induction, ON edema had

resolved (Fig. 4C). There was loss of the RGC axonal component of the intraretinal ON (Fig. 4C, arrow) with shrinkage of the apparent ON diameter. The intraorbital portion of the ON also showed increased cellularity centrally, suggesting ON remodeling (Fig. 4C, double arrows).

At higher magnification, the control retinal section (Fig. 4D) showed a closely packed layer of RGCs, with normal INL and ONL. The INL typically had 3 to 6 layers, whereas the ONL had 8 to 11 layers (Fig. 4D). No retinal histologic changes were seen 37 days after exposure to laser illumination alone (Fig. 4E). In contrast, 37 days after rAION induction (Fig. 4F), morphologic retinal changes are apparent in the RGC layer, with a reduction in the number of RGC nuclei. RGC loss was visible as an increased spacing of RGCs, without loss of either INL or ONL layer thickness (Fig. 4F; compare RGC, INL, and ONL with those in Figs. 4D and 4E).

Quantification of average RGC nuclei in rAION-affected and different control retinas ($n = 5$ animals) is shown in Figure 5. There was no difference in the average number of nuclei in the INL and ONL between any of the treated or naïve groups (measured as the total nuclear thickness, rather than individual nuclei (11.3 ± 0.7 layers for ONL; 3.9 ± 0.3 layers for INL).

Analysis revealed a 40.8% average decline in the number of RGCs for all rAION eyes (Fig. 4; RGC: 34.2 ± 4.3 [SD] for RB-treated control vs. 20.3 ± 5.0 in AION-treated). This decrease is statistically significant (Student's two-tailed t-test; $P < 0.005$). In comparison, there was no significant change in the number of RGCs between RB-treated controls and laser-treated (no RB) controls, compared with the number of RGCs in naïve (no laser/no dye) age-matched control animals (Fig. 5; RGC; compare first three bars). That there was no significant change
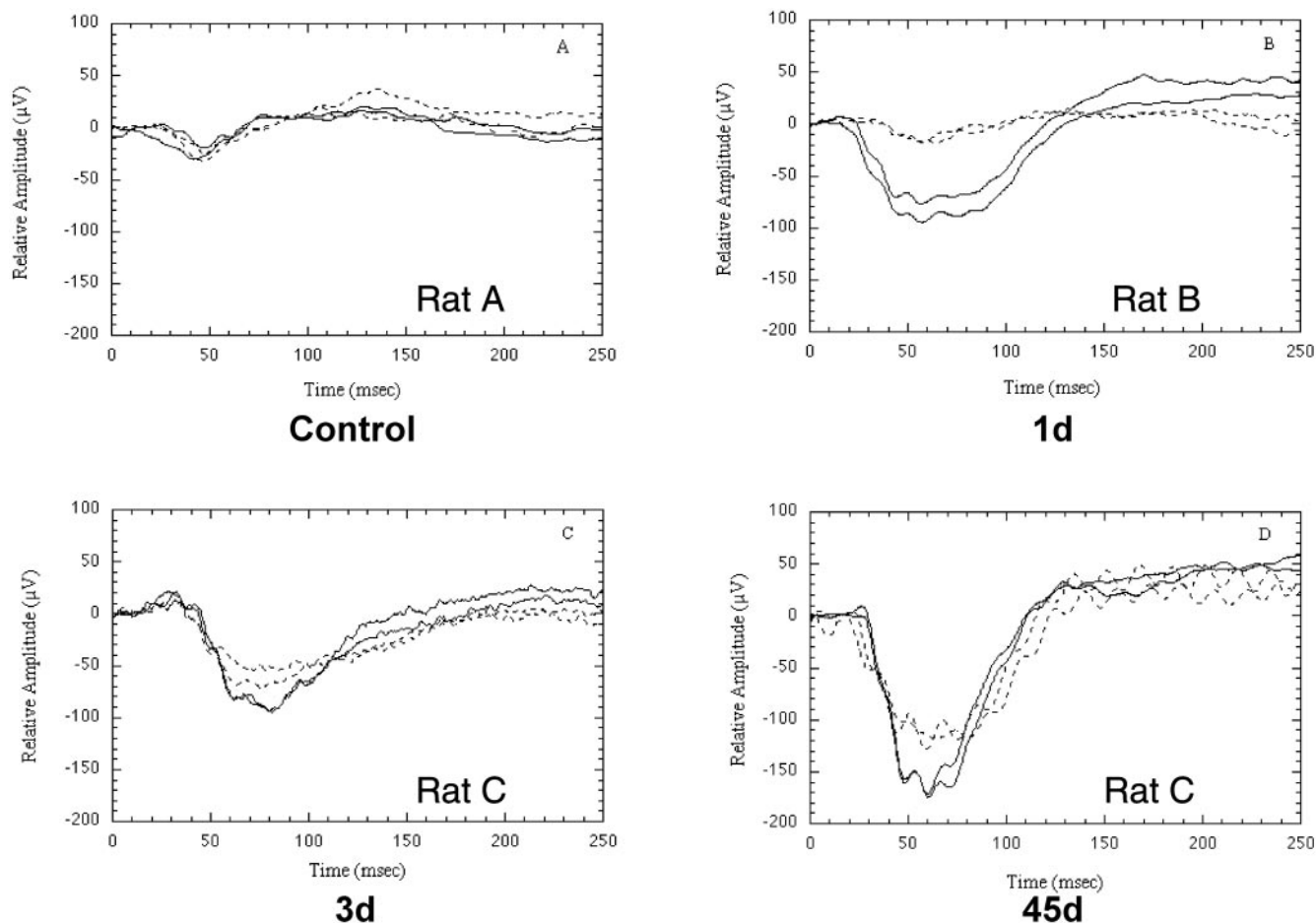
FIGURE 3. ON functional response after rAION. rAION was induced in the right (experimental) eye of each rat, and the left eye was used as an untreated control. Animals were allowed to recover for different times. VEPs were recorded from treated (experimental) and contralateral (control) eyes. Results are shown for each eye. Differences in amplitude between individual panels are not comparable. In all panels, *solid traces* represent the control (left) eye, *dotted traces* the experimental (right) eye. The two similar traces in each panel represent duplicate testing procedures on each eye, consisting of 80 averaged responses. (**A**) Responses in an animal 1 day after laser irradiation/no photoinducible dye in one eye (positive control). There was no VEP amplitude difference apparent between the two eyes. (**B**) A large response produced by maximum rAION induction, 1 day after treatment. (**C**) VEP response 3 days after rAION induction. A 23% to 28% decrease in amplitude occured in the experimental eye. (**D**) Long-term changes in the same rat (rat C) 45 days after rAION induction. The experimental eye continued to have an approximate 23% to 28% decrease in measurable amplitude.

in number of RGCs in all controls (Fig. 5; naïve; RB only, and laser/no RB) implies that the rAION-induced loss of RGCs is a direct result of the combination of RB+laser induction, rather than of purely laser-induced thermal effects or RB-induced toxicity.

Axonal Changes in ON Sections after rAION Induction

The normal (control) ON (Fig. 6A) contained regular axon bundles, with tightly packed myelinated large and small-caliber axons (Fig. 6A, Ax). At 6 days, There was also swelling and increased staining of individual axons (Fig. 6B, double arrows), suggesting either axonal swelling or edema. Eleven days after induction, there was axonal collapse, with disruption of normal architecture (Fig. 6C, arrow). Axon loss and stromal scarring were apparent 90 days after induction of rAION (Fig. 6D, asterisk). Post-rAION axonal loss in the ON was typically central, with sparing of the peripheral RGC axons (Fig. 6E). Thus, both early and long-term functional and histologic changes occurred after induction of rAION that are similar to those in the human disease.[3,24]

rAION-Induced Changes in Retinal Gene Expression

Identifying early retinal gene responses to rAION can suggest pathways critical for RGC stress, cell death commitment, and retinal homeostasis. Analyses of retinal gene expression of selected genes are shown in Fig. 7. Retinal c-fos expression rapidly increased after rAION induction, with c-fos mRNA levels five times higher than in the contralateral (control) eyes 5 hours after rAION induction (Fig. 7A; 5.7% ± 3.5% [SD]). c-Fos levels were equivalent in both eyes 7 days after induction (1.0% ± 0.5%). The rAIO- induced early increase in c-fos expression is statistically significant (Student's two-tailed t-test; $P < 0.05$). No observable difference in c-fos expression occurred between sham-treated (laser light alone) and control eyes 1 day after sham rAION induction (data not shown). Brn 3.2 mRNA levels declined 1 day after induction to ~50% of control (contralateral) levels (Fig. 7D; −0.5% ± 0.2% SD), and remain at half of the control value (−0.5% ± 0.3% SD) at 7 days after induction. The 50% decline in brn 3.2 mRNA correlates well with the later (~40%) RGC decrease in rAION-treated
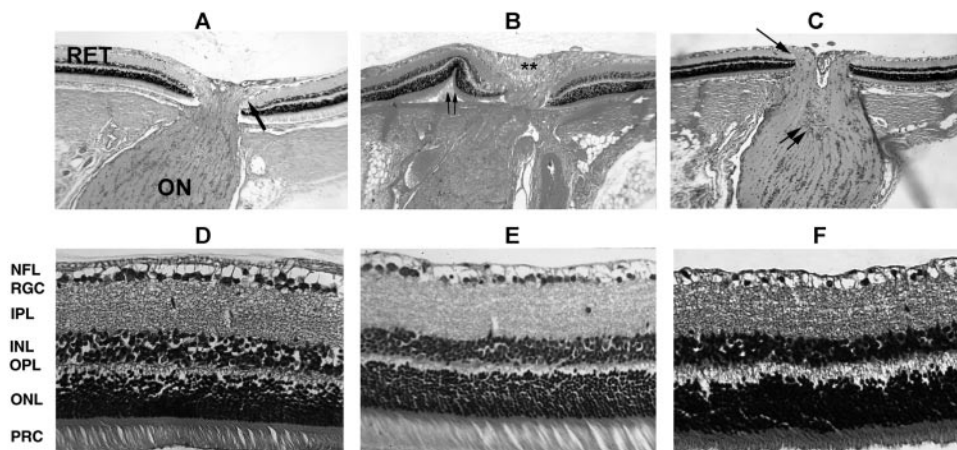
Figure 4. rAION-induced retina and ON histologic changes in the rat. (**A**) Appearance of the sham-treated (laser control/no dye) retina at the retina–ON junction 1 day after treatment. The retina–ON junction is flat against the retina. The RGC axons in the intraretinal portion of the ON form a triangular structure (*arrow*). (**B**) Appearance of the retina–ON junction 1 day after rAION induction. ON edema was apparent by the displacement of the peripapillary retina (*double arrows*) and increased substance in the intraretinal portion of the ON (**★★**). (**C**) Appearance of the retina–ON junction 37 days after rAION induction. The intraretinal portion of the ON was shrunken in substance, with straightening and reduction in the width of the RGC axonal layer (*arrow*). There was also increased cellularity centrally in the substance of the ON (*double arrow*). (**D**) Appearance of the naïve (no RB dye/no laser) retina. RGCs were closely packed in a single layer. (**E**) Appearance of sham-treated laser control retina 37 days after treatment. No change in the number of RGC nuclei was seen. Other cell layers were unchanged in appearance. (**F**) Appearance of the retina 37 days after rAION induction. The number of nuclei in the RGC layer was markedly reduced. Magnification: (**A, B, C**) ×100; (**D, E, F**) ×200.

retinas (see Fig. 5; RGCs in rAION-treated vs. control eyes). Little if any alteration in outer retinal cell function occurred, as measured by the photoreceptor-specific gene opsin mRNA, between induction and 7 days after induction (Fig. 7E; opsin; 0 days, 1.1% ± 0.2%, and 7 days, −0.2% ± 0.1%). Changes in HSP90 isoform mRNA expression levels are not statistically significant (data not shown). There was a trend for HSP86 (Fig. 7C) and -84 (Fig. 7F) to increase over uninduced retinas from 3 to 7 days (compare Fig. 7C: HSP86, 3–7 days; Fig. 7F: HSP84, 3–7 days). HSP70-1/2 mRNA expression is stable after induction for the first 2 days (1.0% ± 0.2% at 0 days vs. − 0.1% ± 0.2% at day 2; Fig. 7B, HSP70-1/2), with a possible slight increase at 3 days after rAION (Fig. 7B; HSP70-1/2, 3 days, 1.3% ± 0.7%). HSP70-1/2 levels were at baseline 7 days after induction (Fig. 7B; HSP70-1/2; 7 days, 1.0% ± 0.3%).
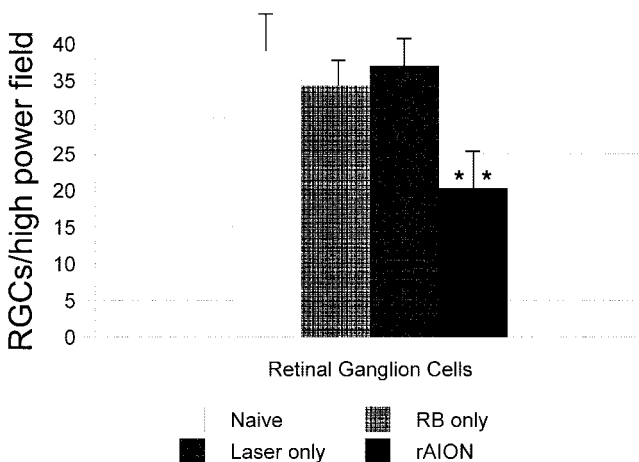

Figure 5. Long-term changes in the number of retinal cells in naïve (untreated), dye-treated, and laser-treated controls and rAION-treated eyes 37 days after treatment. After fixation and hematoxylin-eosin staining of 6-μm sections, cell nuclei in the ONL and INL, and the number of individual nuclei in the RGC layer per high power field (×400) were counted in individual sections. Twelve sections per retina were averaged (n = 5 animals/group). Results are expressed as the mean ± SD. Naïve: no dye/no laser; RB control: dye/no laser; laser control: laser/no RB dye; and rAION-induced: RB dye+laser retinas. RGC loss was present in rAION-induced retinas only. **Significant difference (P < 0.005).

rAION-Associated Changes in Retinal Protein Localization and Expression

mRNA alterations did not necessarily correspond to changes at the protein level. Immunohistological analysis of brn 3.2, HSP86, and HSP84 protein in the retina showed subtle changes after rAION treatment (Fig. 8). A strong brn 3.2 signal was present in control RGC nuclei (Fig. 8A; RGC: arrows). The brn 3.2 signal decreased in many RGCs by 3 days after rAION induction (Fig. 8B) and disappeared in many RGCs 7 days after rAION induction. A reduced number of RGCs were positive for this protein (Fig. 8C, arrow).

Both HSP84 and-86 are found in the retina, but are concentrated in different intraretinal regions, suggesting differential expression by different retinal cell types. HSP86 is present in cell nuclei,[25] whereas HSP84 is present in both the nuclear and cytoplasmic compartments.[25] Strong HSP86 expression occurred in RGC nuclei of control retinas (Fig. 8D, double arrows) and in the OPL. Three days after induction, HSP86 protein signal increased in a few RGC nuclei, but decreased in many others (Fig. 8E; RGC; compare with 8D). There was a loss of discrete HSP86 signal in the OPL at 3 days (Fig. 8E), and reformation at 7 days (Fig. 8F), suggesting that HSP86 may be reactively mobilized or synthesized in RGC-associated retinal interneurons and glia after rAION or may be a generalized reactive retinal response to changes occurring in RGCs. No changes were seen in sham- or RB-treated eyes (data not shown). Few RGCs expressed HSP86 7 days after AION induction (Fig. 8F, double arrow).

Strong HSP84 protein signal was present in the RGC layer and inner segment of the photoreceptor layer in control retina (Fig. 8G). Three days after rAION induction, there was an accumulation of HSP84 protein in the NFL (Fig. 8H). By 7 days after induction, HSP84 signal declined in the NFL and RGC layer (Fig. 8I). There was increased HSP84 staining in the inner plexiform layer (IPL; Fig. 8I, double arrow), suggesting that reactive changes continue in RGC layers.

DISCUSSION

rAION resembles human AION functionally and morphologically. The changes in rAION are therefore likely to be similar to those in human disease. Because RGCs are typical long-axon CNS neurons, the rAION model may be appropriate for in vivo
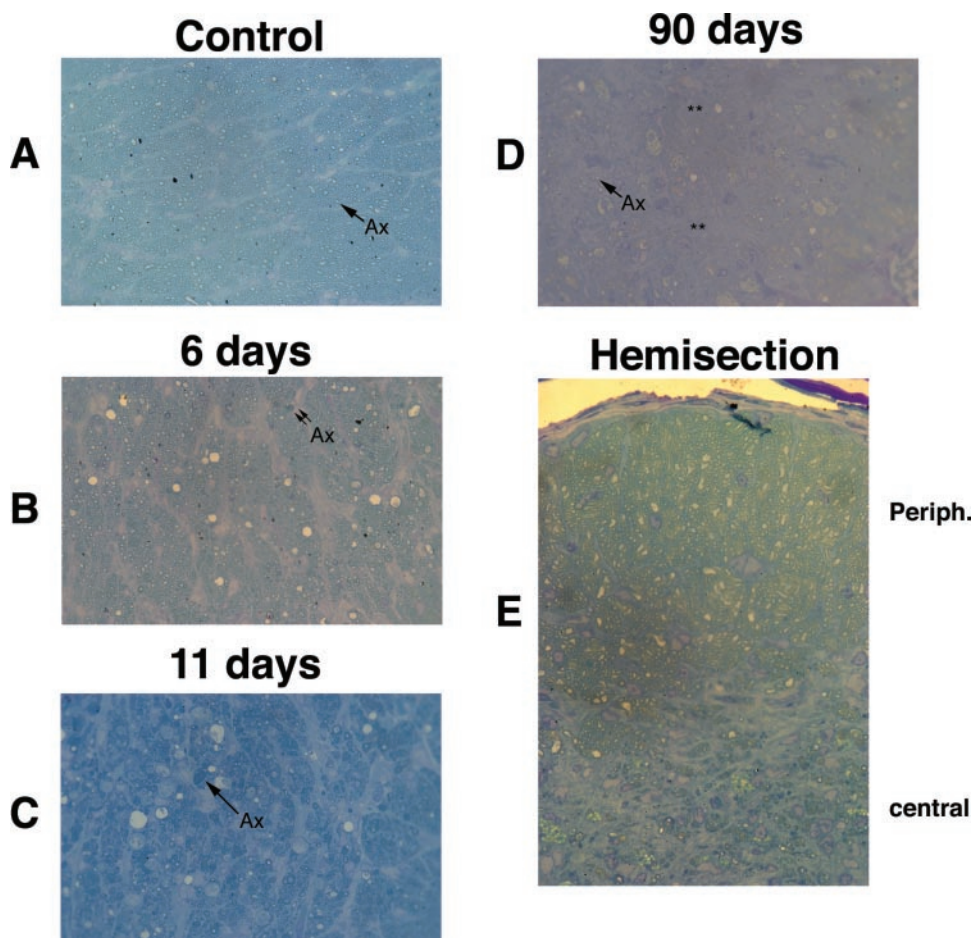
FIGURE 6. Effect of rAION on the rat ON. ON sections were embedded in Epon, and sections (0.5 μm) were stained with toluidine blue. (**A**) Appearance of the normal (control) ON. *Arrow*: Axons (Ax). (**B**) ON appearance 6 days after induction of rAION. Some axons showed increased staining, suggesting axonal collapse or edema (*double arrow*). There were numerous cystic spaces or vacuoles. (**C**) ON appearance 11 days after rAION. Most axons were collapsed and filled with blue-stained material (*arrow*). The remaining patent axons were swollen. (**D**) ON appearance 90 days after rAION. Remaining axons had markedly variable diameters and thickening was evident (★★). (**E**) Appearance of one half of the ON (hemisection) after rAION. Peripheral and central nerve regions are indicated. There was a loss of axons centrally, with axonal sparing and largely intact axons in the peripheral nerve. Magnification: (**A–D**) ×1000; (**E**) ×160.

study of CNS axonal ischemic disorders, such as lacunar strokes, ischemic auditory neuropathy, and AION.[26–28]

After rAION induction, there was a rapid (within 30 minutes) loss of circulation to the ON. rAION-induced edema peaked 1 to 2 days after induction, and resolved by 5 days, whereas human AION-induced ON edema resolves by 4 weeks.[20] Despite early resolution of ON edema, ON function was compromised by 3 days after rAION induction, and VEP amplitude remained depressed even 37 days after induction. rAION grossly resulted in a pale, shrunken ON, similar to that seen clinically in human AION.[20] The late ON changes were coincident with a loss of ~40% of nuclei in the RGC layer. Similar to human AION, rAION specifically altered the number of RGC layer cells without grossly changing the number of cells in the INL and ONL.[3] No cellular changes were visibly apparent in the ONL or INL levels 37 days after rAION induction (Fig. 4F), and there were no quantitative changes in INL or ONL thickness. The rAION-induced cellular losses were largely limited to the RGC layer and are statistically significant. Thus, similar to human AION,[20,23,29] rAION produced early functional changes and permanent retinal and ON alterations.

rAION-induced histologic ON changes were apparent 6 days after induction in the rat ON, with axonal swelling and collapse. Myelin sheath breakdown (demyelination) was prominent by day 11. Failure of axonal integrity was thus concurrent with neuronal somatic changes early in the course of rAION. Permanent changes included septal thickening and axonal loss. These changes were most noticeable in the ON center, which represents the vascular "watershed," and is also typical of human AION.[2,28] The central loss results suggest that damage in rAION is due to ischemia resulting from preferential damage

of the terminal capillaries supplying the nerve center, rather than from a nonspecific effect of dye or thermal toxicity, because the latter two responses would be predicted to have a random effect on axons scattered throughout the ON. The central axonal loss is similar to that reported in many cases of human AION.[30] Thrombosis induced by artificially damaging the vascular endothelium, using RB-induced superoxide radicals, could also lead to local effects on RGC axons that are distinct from those caused by natural microvascular occlusion (for example, by release of soluble factors). However, these questions are beyond the scope of the present study.

rAION was used to identify potential retinal gene responses that may be analogous to those occurring in clinical AION. Gene expression results, except for c-fos, though not statistically significant, are suggestive of specific trends. The minimal changes in photoreceptor-specific gene expression suggest that rAION's effects are largely limited to the inner retinal cell layers. The mRNA for c-fos, an immediate-early response gene, through elevated over baseline for the first 3 days after induction, showed two peaks of induction: one at 5 hours after rAION induction, and another at 2 to 3 days. c-Fos expression then declined to baseline 7 days after induction. Strong c-fos expression occurs in other animal models after CNS ischemia, pain, and surgical axotomy,[31–33] suggesting that some similarities exist in a variety of CNS stress responses. The bimodal response suggests that, similar to brain,[33] there may be at least two distinct response periods after rAION-induced retinal stress.

Brn 3.2 mRNA levels rapidly declined, with a plateau 1 day after induction, compared with the uninduced eye, and remained low up to 7 days in rAION retinas. A decline in Brn 3.2
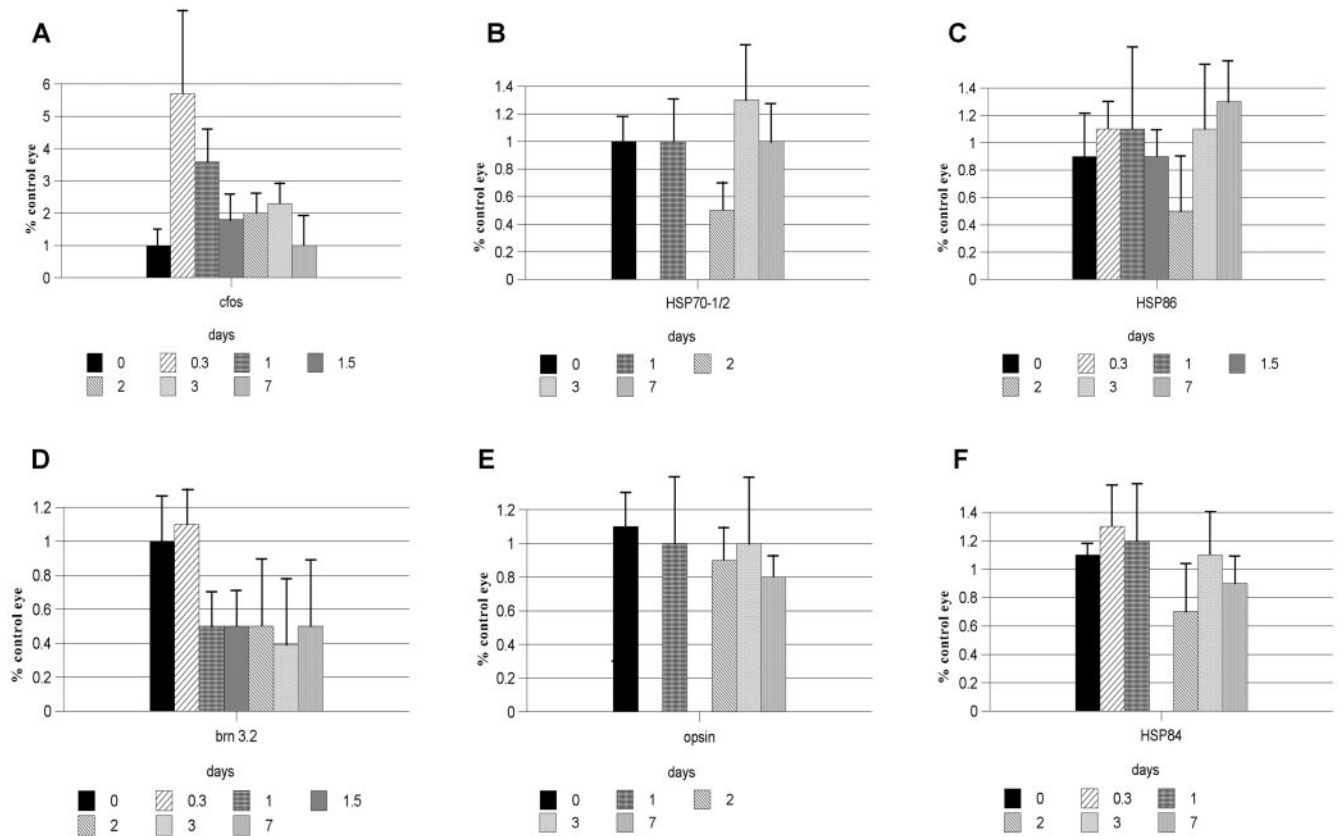
FIGURE 7. rAION-induced changes in rat retinal gene expression. rAION was induced in one eye of each animal, with the contralateral eye used as a control. After rAION induction, total retina RNA was isolated at different times ($n = 5$ animals per time point). Semiquantitative, two-stage rt-PCR was performed on total RNA from rAION and control eyes, with expression compared between experimental and control eye pairs. Each data pair was considered a single experiment. Individual bars for each time point are the mean $\pm$ SD of results in five animals. The difference is compared with the contralateral (control) retina set at 100% (1.0), on the ordinate. (**A**) c-Fos, (**B**) HSP70-1/2, (**C**) HSP86, (**D**) brn 3.2, (**E**) rhodopsin (opsin), and (**F**) HSP84.

protein was histologically and quantitatively apparent 3 days after induction of rAION. Brn 3.2 expression in the retina is largely restricted to RGCs and is associated with RGC survival, and its loss results in RGC apoptosis.[34] The loss of Brn 3.2 activity is explainable by the relative RGC specificity of Brn 3.2 and the decline in RGC-specific functions after rAION. The long-term decrease in retinal expression of Brn 3.2 probably represents RGC functional reprogramming.

There was a trend toward a decline in retinal HSP86 mRNA that was at its maximum by 2 days after induction and returned to normal control levels 3 to 5 days after induction. Although HSP84 mRNA levels also suggest a bimodal retinal response, these changes were small (20%–40% differences) and are not significant. The later increase in HSP86 expression suggests a possible retinal reactive response to RGC axonal ischemia, which is supported by the late (2–3 days) increase in the retinal mRNA levels for the classic stress-response gene HSP70-1/2. Increased RGC-HSP90 expression has also been shown after transient ischemia.[35] HSP86 expression is known to increase selectively after stress in a number of other systems, whereas HSP84 is constitutively expressed.[36] Although the experimental sample numbers were small, sample trends suggest that retinal gene expression changes occur after rAION and that some of these changes may be biphasic. Biphasic genetic response to traumatic and ischemic CNS injury has been observed.[33] Thus, the retina probably modifies its genetic programming rapidly after rAION, to respond to RGC axonal ischemic stress. This hypothesis is supported by the immunochemical changes at the cellular level.

It is evident that there was immunohistological changes in retinal expression of the HSP90 isoform after rAION, although total quantitative HSP90 expression was relatively stable. The latter finding may be explained by the fact that HSP90 proteins are used by all retinal cells, but at relatively different levels and for different functions. HSP90 mRNA and proteins are differentially expressed by RGCs, for axon-intensive functions.[18] HSP84 and -86 proteins apparently accumulated in the RGC and NFL layers of the retina up to 3 days after induction. RGC-specific HSP90 isoform expression was considerably reduced at 7 days after rAION. Other (non-RGC) retinal cell types also showed a change in HSP90 expression after rAION. HSP90 isoform signal in control retina was present in the RGC, OPL, and photoreceptors (Prcs). After rAION induction, HSP84- and -86 signal declined at 3 days in the OPL and was reconstituted by 7 days after induction. HSP84 expression may also selectively increase at 3 and 7 days in the INL and IPL. The later changes in HSP90 isoform protein expression in the retina may be a result of non-RGC, stress-associated HSP90 functions that are distinct from their RGC-specific functions. The complex immunohistologic pattern of retinal HSP90 redistribution after ischemic axonopathy, suggests that HSP90 isoforms may perform multiple functions in different retinal cell types.

Our model may differ from the human disorder, in that microvascular occlusion in the model is produced by superoxide radicals, whereas the mechanism of "natural" vascular occlusion in human AION is unknown. Nevertheless, the changes observed after induction of rAION imply that a well-defined sequence of early responses occur after CNS ischemic ax-

FIGURE 8. rAION-induced immuno-histochemical changes in RGC-expressed proteins. Brn 3.2 expression in (**A**) control retinas. Brn 3.2 signal was limited to the RGC nuclei (*arrows*); (**B**) RGCs 3 days after rAION induction; and (**C**) in rAION-treated retina 7 days after induction. There was a loss of brn 3.2 signal in many RGC nuclei, with continued strong expression in other RGC nuclei (*arrow*). (**D**) HSP86 expression in control retina, showing strong HSP86 expression in RGC nuclei (*double arrow*), as well as in the OPL. HSP86 expression in rAION-treated retinas (**E**) 3 days after induction, showing decreased RGC HSP86 signal and increased INL signal, suggesting HSP86 mobilization, and (**F**) 7 days after induction, showing loss of HSP86 in many RGC nuclei, with continued strong expression in scattered RGCs (*double arrow*). HSP86 signal in the IPL had reconstituted. (**G**) HSP84 expression in control retina in RGC nuclei (*arrow*) and in the OPL and Prc layers. HSP84 expression in rAION retina (**H**) 3 days after induction showing accumulation in RGC and NFL layers (*arrow*); and (**I**) 7 days after induction showing reduced expression in RGCs is, with increased signal in the IPL (*double arrow*). Magnification, ×400.
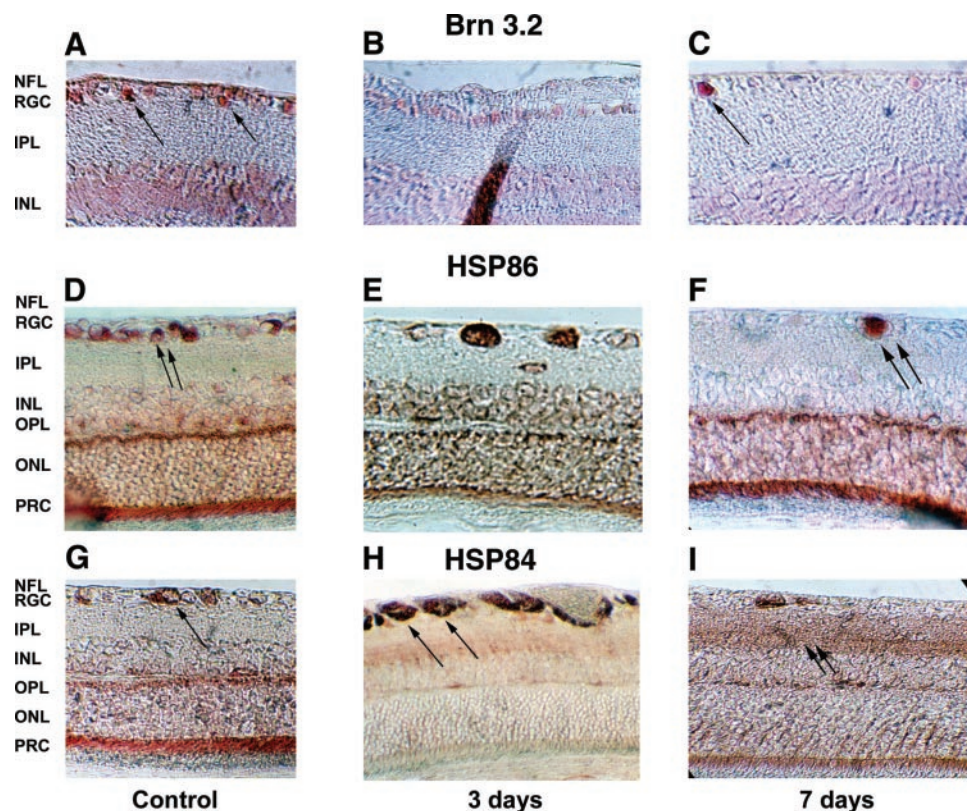
onopathy and that irreversible changes may begin within 1 day after axonal ischemia, despite adequate neuron soma vascularization. These early changes probably prime the retina for the later cascade of events related to rAION-induced RGC death. The rAION model can enable a detailed analysis of the individual retina and ON changes occurring after ON stroke, which may be useful in determining possible therapeutic interventions for this disorder.

References

1. Dacheux RF, Raviola E. Functional anatomy of the retina. In: Albert DM, Jakobiec FA, editors. *Principles and practice of Ophthalmology.* Baltimore: WB Saunders 1994;285–309.
2. Hayreh SS. Anterior Ischemic optic neuropathy. I. Terminology and pathogenesis. *Br J Ophthalmol.* 1974;58:955–963.
3. Levin LE. Apoptosis of retinal ganglion cells in anterior ischemic optic neuropathy. *Arch Ophthalmol.* 1996;114:488–491.
4. Selles-Navarro I, Ellezam B, Fajardo R, Latour M, Mckerracher L. Retinal ganglion cell and non neuronal cell responses to a microcrush lesion of adult rat optic nerve. *Exp Neurol.* 2001;167:282–289.
5. Krueger-Naug AM, Emsley JG, Myers TL, Currie RW, Clarke DB. Injury to retinal ganglion cells induces the expression of the small heat shock protein HSP27 in the rat visual system. *Neuroscience.* 2002;110:653–665.
6. Johnson EC, Deppmeier LM, Wentzien SK, Hsu I, Morrison JC. Chronology of optic nerve head and retinal responses to elevated intraocular pressure. *Invest Ophthalmol Vis Sci.* 2000;41:431–442.
7. Cioffi GA, Orgul S, Onda E, Bacon DR, Van Buskirk EM. An in-vivo model of chronic optic nerve ischemia: the dose- dependent effects of endothelin-1 on the optic nerve vasculature *Curr Eye Res.* 1995;14:1147–1153.
8. Rodgers MAJ. Light-induced generation of singlet oxygen in solutions of rose bengal. *Chem Phys Lett.* 1981;78:509–514.
9. Mosinger JL, Olney JW. Photothrombosis-induced ischemic neuronal degeneration in the rat retina. *Exp Neurol.* 1989;105:110–113.
10. Kikuchi S, Umemura K, Kondo K, Saniabadi AR, Nakashima M. Photochemically induced endothelial injury in the mouse as a screening model for inhibitors of vascular intimal thickening. *Arterioscler Thromb Vasc Biol.* 1998;18:1069–1078.
11. Ocho S, Iwasaki S, Umemura K, Hoshino T. A new model for investigating hair cell degeneration in the guinea pig following damage of the stria vascularis using a photochemical reaction. *Eur Arch Otorhinolaryngol.* 2000;257:182–187.
12. Wilson CA, Hatchell DL. Photodynamic retinal vascular thrombosis. *Invest Ophthalmol Vis Sci.* 1991;32:2357–2365.
13. Pooler JP, Valenzeno DP. Physicochemical determinants of the sensitizing effectiveness for photoxidation of nerve membranes by fluorescein derivatives. *Photochem Photobiol.* 1979;30:491–498.
14. Luna MC, Wong S, Gomer CJ. Photodynamic therapy mediated induction of early response genes. *Cancer Res.* 1994;54:1374–1380.
15. Grimm C, Wenzel A, Hafezi F, Reme CE. Gene expression in the mouse retina: the effect of damaging light. *Mol Vis.* 2000;6:252–260.
16. Turner EE, Jenne KJ, Rosenfeld MG. Brn-3.2: a Brn-3-related transcription factor with distinctive central nervous system expression and regulation by retinoic acid. *Neuron.* 1994;12:205–218.
17. Holbrook NJ, Udelsman R. Heat shock protein gene expression in response to physiologic stress and aging. In: Morimoto RI, Tissieres A, Georgopoulos C, eds. *The Biology of Heat Shock Proteins and Molecular Chaperones.* Cold Spring Harbor, NY: Cold Spring Harbor Press;. 1994;577–593.

18. Bernstein SL, Russell P, Wong P, Fishelevich R, Smith LEH. Heat shock protein 90 in retinal ganglion cells: association with axonally transported proteins. *Vis Neurosci.* 2001;18:429–436.

19. Rex TS, Lewis GP, Geller SF, Fisher SK. Differential expression of cone opsin mRNA levels following experimental retinal detachment and reattachment. *Mol Vis.* 2002;8:114–118.

20. Hayreh SS. Anterior ischaemic optic neuropathy. II. Fundus on ophthalmoscopy and fluorescein angiography. *Br J Ophthalmol.* 1974;58:964–980.

21. Morrison JC, Johnson EC, Cepurna WO, Funk RH. Microvasculature of the rat optic nerve head. *Invest Ophthalmol Vis Sci.* 1999;40:1702–1709.

22. Sobolewski P, Stankiewicz, A. Evaluation of visual evoked potentials in partial optic nerve atrophy [in Polish]. *Klin Oczna.* 1997;99:299–302.

23. Brigell MB. The visual evoked potential. In: Fishman GA, Birch DG, Holder GE, Brigell MG, eds. *Electrophysiologic Testing.* San Francisco: The Foundation of the American Academy of Ophthalmology; 2001;237–279.

24. Beck RW, Servais GE, Hayreh SS. Anterior ischemic optic neuropathy IX: cup to disk ratio and its role in pathogenesis. *Ophthalmology.* 1987;94:1503–1508.

25. Perdew G, Whitelaw ML. Evidence that the 90-kDa heat shock protein (HSP90) exists in cytosol in heteromeric complexes containing HSP70 and three other proteins with M_r of 63,000, 56,000 and 50,000. *J Biol Chem.* 1997;266:6708–6713.

26. Weisberg LA, Strub RL, Garcia CA. Stroke. In: Weisberg LA, ed. *Essentials of Clinical Neurology.* Baltimore: University Park Press; 1983;147–166.

27. Ishii T, Toriyama M. Sudden deafness with severe loss of cochlear neurons. *Ann Otorhinolaryngology.* 1977;86:541–546.

28. Sadun AA. Optic atrophy and papilledema. In: Albert DM, Jakobiec FA, eds. *Fundamentals of Ophthalmology: Basic and Clinical Practice.* Baltimore: WB Saunders; 1995:2529–2538.

29. Miller N. Anterior ischemic optic neuropathy. In: Miller NR, ed. *Walsh and Hoyts Neuro-ophthalmology.* Baltimore: Williams and Wilkins; 1982;212–226.

30. Knox DL, Kerrison JB, Green WR. Histopathologic studies of ischemic optic neuropathy. *Trans Am Ophthalmol Soc.* 2000;98:203–202.

31. Curran T, Morgan JI. Fos: an immediate-early transcription factor in neurons. *J Neurobiol.* 1995;26:403–412.

32. Mitsikostas DD, Sanchez del Rio M. Receptor systems mediating c-fos expression within the trigeminal nucleus caudalis in animal models of migraine. *Br Res Revs.* 2001;35:20–35.

33. Liu JS, Chang YY, Chen WH, Chen SS. Delayed transhemispheric c-fos gene expression after focal cerebral ischemia-reperfusion in rats. *J Formosa Med Assoc (Taiwan).* 1995;94:649–654.

34. Gan L, Wang SW, Huang Z, Klein WH. POU domain factor Brn-3b is essential for retinal ganglion cell differentiation and survival but not for initial cell fate specification. *Dev Biol.* 1999;210:469–480.

35. Caprioli J, Kitano S, Morgan JE. Hyperthermia and hypoxia increase tolerance of retinal ganglion cells to anoxia and excitotoxicity. *Invest Ophthalmol Vis Sci.* 1996;37:2376–2381.

36. Hansen LK, Houchins JP, O'Leary JJ. Differential expression of HSC70, HSP70, HSP90α, and HSP90β mRNA expression by mitogen activation and heat shock in human lymphocytes. *Exp Cell Res.* 1991;192:587–596.